Article

Simulated Changes in Tropical Cyclone Size, Accumulated Cyclone Energy and Power Dissipation Index in a Warmer Climate

Michael Wehner 🆔

Lawrence Berkeley National Laboratory, Berkeley, CA 94720, USA; mfwehner@lbl.gov

Abstract: Detection, attribution and projection of changes in tropical cyclone intensity statistics are made difficult from the potentially decreasing overall storm frequency combined with increases in the peak winds of the most intense storms as the climate warms. Multi-decadal simulations of stabilized climate scenarios from a high-resolution tropical cyclone permitting atmospheric general circulation model are used to examine simulated global changes from warmer temperatures, if any, in estimates of tropical cyclone size, accumulated cyclonic energy and power dissipation index. Changes in these metrics are found to be complicated functions of storm categorization and global averages of them are unlikely to easily reveal the impact of climate change on future tropical cyclone intensity statistics.

Keywords: tropical cyclones; climate change; accumulated cyclone energy index; power dissipation index

1. Introduction

With the development of the HighResMIP subproject of the 6th version of the Coupled Model Intercomparison Project, the multi-decadal simulation of global and basin scale tropical cyclone statistics has become mainstream [1]. These models, with horizontal resolutions ranging from 50–20 km can be considered "tropical cyclone permitting" or at least "tropical cyclone-like permitting" as storms are produced in these simulations that bear some similarities to actual tropical cyclones, such as high radial winds, low central pressures and warm central cores [2–7]. Observed patterns and seasonality of cyclogenesis and resulting cyclone tracks can be reasonably reproduced using prescribed sea surface temperatures as a lower boundary condition [5,8] with errors in these statistics manifested by a variety of factors often traceable to subgrid parameterizations. Indeed, as high performance computing platforms edge towards the exascale, some of these model deficiencies, in particular parameterized deep cumulus convection processes, can be ameliorated by yet further increases in horizontal resolution [9].

However, given current computational limitations, HighResMIP-class models are the currently available tool to perform the multi-realization, multi-decadal simulations able to inform about the effect of global warming on tropical cyclone statistics. A recent pair of expert team studies notes that there remains much uncertainty about detectible and attributable changes in observed tropical cyclone statistics [10], even in their projected future changes under significantly more warming than has occurred to date [11]. The first report finds that an observed poleward shift of tropical cyclones in the Northwestern Pacific is "highly unusual compared to expected natural variability" but casts doubt on whether any other observed tropical cyclone properties are detectable, much less attributable to anthropogenic climate change. However, a number of other event attribution studies found that precipitation in individual tropical cyclone has been increased due to warmer sea surface temperatures with low estimates of scaling with temperature increases, according to the Clausius–Clapeyron relationship and best estimates of significantly higher scaling [12–17]. While these studies are not formal detection and attribution studies, confidence that there is a human influence on tropical cyclone precipitation is enhanced by the demonstration

that eastern US hurricane precipitation patterns and magnitude can be well represented by models at HighResMIP-class resolutions [18] and in general by previous detection and attribution studies on extreme precipitation [19,20]. Event attribution changes have also investigated anthropogenic changes in tropical cyclone wind speeds [17,21] with very clear future increases but less conclusive findings about the influence at current warming levels [22].

Projections from HighResMIP-class models suggest profound changes in tropical cyclone statistics but with significant uncertainties. The intensity of the most powerful storms, as measured by instantaneous maximum wind speed or minimum central pressure, increases in nearly all of these models with warmer temperatures [5,23–25]. This is very carefully stated in the expert team assessment by Knutson et al. (2019) [11]. As "For TC intensity, 10 of 11 authors had at least medium-to-high confidence that the global average will increase. The mechanism for such a change is straightforward. Intense tropical cyclones occur when ambient wind shear is low and humidity and sea surface temperatures are high. As there will be periods in future warmer climates where wind shear is favorably low, a larger amount of latent and sensible heat energy is available for the storm's kinetic energy. However, this very carefully crafted statement reflects the uncertainty in the number of future tropical storms. Most of the HighResMIP-class models project a decrease in the total number of tropical storms with global warming. But there is substantial variability across models and if the decrease in total number of storms is very large, the number of intense storms may decrease. Hence, another way of stating the expert team assessment is that the fraction of intense tropical cyclones across all tropical storms is expected to increase whether or not the actual number of intense storms increases or decreases. However, the fraction of storms deemed intense is not particularly relevant to impacts, thus motivating this study to examine intensity metrics with nonlinear dependences on peak wind speed.

While the Saffir–Simpson category scale is routinely used to communicate to the public the imminent danger posed by tropical cyclones, more comprehensive alternative scales have been proposed but not widely adopted [26–28]. While interpreted by the impact of selected damage types, the Saffir–Simpson scale is actually defined by 1 min average peak near surface wind exceedances over fixed thresholds. From a detection and attribution point of view, this selection of a pointwise peak from an effectively instantaneous and pointwise quantity may be too noisy to readily ascertain any human influence on tropical cyclone intensity until global warming levels are much larger than present.

In this paper, a selection of other metrics of tropical cyclone intensity are examined with attention paid to their changes as temperatures increase, if any. Projections of future responses to global warming levels larger than that currently realized in the real world can inform us to what changes to expect or at least what to look for in the observations. For these purposes, this study uses simulations from a tropical cyclone permitting model with a strong negative response in global tropical cyclone frequency to warmer global temperatures. These metrics, storm size, accumulated cyclone energy and power dissipation index, are chosen to be more integrative of the entire storm lifecycle than simply counting annual storms in each Saffir–Simpson category. The focus here is only on global quantities but it is recognized that the Northwestern Pacific dominates the global average of most tropical cyclone statistics. Indeed, there is no guarantee that tropical cyclone activity will respond to warming by the same amount or direction across different ocean basins as not only is the warming of the ocean non-uniform, the changes in other tropical cyclogenesis precursors are also non-uniform as are the changes in large scale influences on subsequent tropical cyclone paths and development.

2. The CAM5 Climate Model Setup and Its Tropical Storm Frequency Response on the SAFFIR-Simpson Scale to Warming

The community atmospheric model, version 5.1 (CAM5.1) is a global atmospheric general circulation model with prescribed sea surface temperatures and sea ice concentrations (Neale et al., 2012). For this study, it has been run using a finite difference dynamics scheme on a regular latitude–longitude mesh of approximately one quarter-degree or

~25 km [29]. Its simulated global annual tropical cyclone frequency is remarkably close to observations although substantial cyclogenesis biases are exhibited in the Northern Pacific Basin [8]. Simulated global annual tropical cyclone frequency has previously been shown in this model to decrease relative to that of the current climate when driven by conditions approximating the stabilized 1.5 and 2C targets of the Paris Agreement [24]. Figure 1 extends these simulations to include a preindustrial global temperature level and a stabilized 3C above preindustrial temperature target. The experimental protocols including sea surface temperatures and sea ice concentrations for the preindustrial (here denoted "Natural") and a present day period 1996–2015 (here denoted "Historical") come from the Climate of the 20th Century (C20C+) Detection and Attribution Project (available online: portal.nersc.gov/c20c (accessed on 6 September 2021)), designed for event attribution [30]. Experimental protocols for the 1.5 and 2C stabilized climates come from the the Half A degree additional warming, Prognosis and Projected Impacts (HAPPI) project [31] denoted here as HAPPI1.5 and HAPPI2.0 respectively. The sea surface temperature boundary conditions and greenhouse gas concentrations for the 3C stabilized climate were calculated from the CMIP5 models in the same way as HAPPI but suitably adjusted for the warmer temperatures. As all of the warmer climate simulations are stabilized against future emissions, their aerosol concentrations are set at the preindustrial levels. Only the present day simulations differ in this regard. All the tropical cyclone statistics presented here are calculated from storm tracks obtained from TECA2, the toolkit for extreme climate analysis [32].

The observed frequency of named tropical storms of all Saffir–Simpson intensities from tropical storm to category 5 is about 86 storms per year with an interannual standard deviation of 9.6. From Figure 1, the model under observed boundary conditions produces about 73 storms per year with an interannual standard deviation of 9. Multiple realizations of each temperature scenario were produced. Five simulations of the historical period were concatenated resulting in 100 total simulated years, approximating a stable climate. Ensemble sizes of all the configurations are shown as numbers within the bars of Figure 1. The error bars shown in Figure 1 represent the standard errors calculated using these ensemble sizes. Figure 1 shows that the CAM5.1 model exhibits a strong decrease in storm frequency as the climate warms.

The left panel of Figure 2 reveals that this simulated change in storm frequency varies with Saffir–Simpson categories and the bulk of the decrease in total storm frequency stems from the weaker categories of tropical storm (here denoted as category 0) and category 1. Category 5 storms are more frequent in the future warmer climates than in the preindustrial and current climates despite the overall decrease in cyclogenesis. The same statement is true for category 4 when comparing the future to present climates, but the preindustrial climate actually produced more storms in all other categories than the present day climate. This change in the distribution of peak storm intensities will influence changes in other more integrative intensity metrics.

The right panel of Figure 2 shows the variation in the fraction of annual average storm counts across Saffir-Simpson categories for the various global warming levels. This reveals a somewhat clearer climate change signal, especially for intense tropical cyclones and supports the conservative conclusions of the expert team assessment [11]. It is worth mentioning here that the cleanest comparison is between the natural and the future warmer simulations as they all have the same aerosol forcings. Neglecting the historical simulations then, the fractional increase in intense tropical cyclones (Categories 4 and 5) is monotonic with warming.
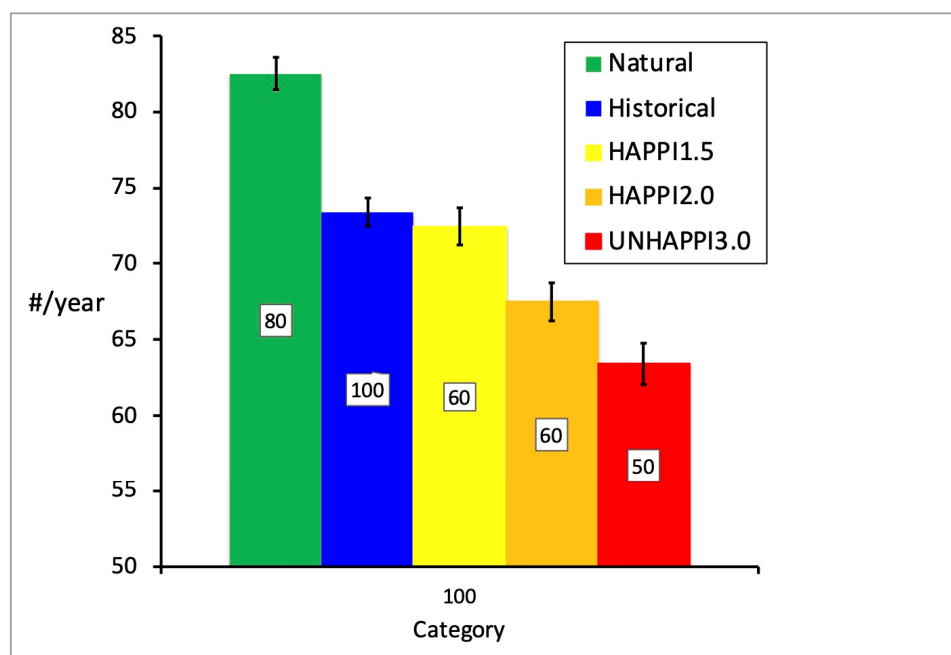
Figure 1. Annual number of all tropical storms (TS-cat5) as simulated by CAM5.1 at various global warming levels. Numbers in the centers are the number of simulated years for each numerical experiment. Error bars indicate standard error.
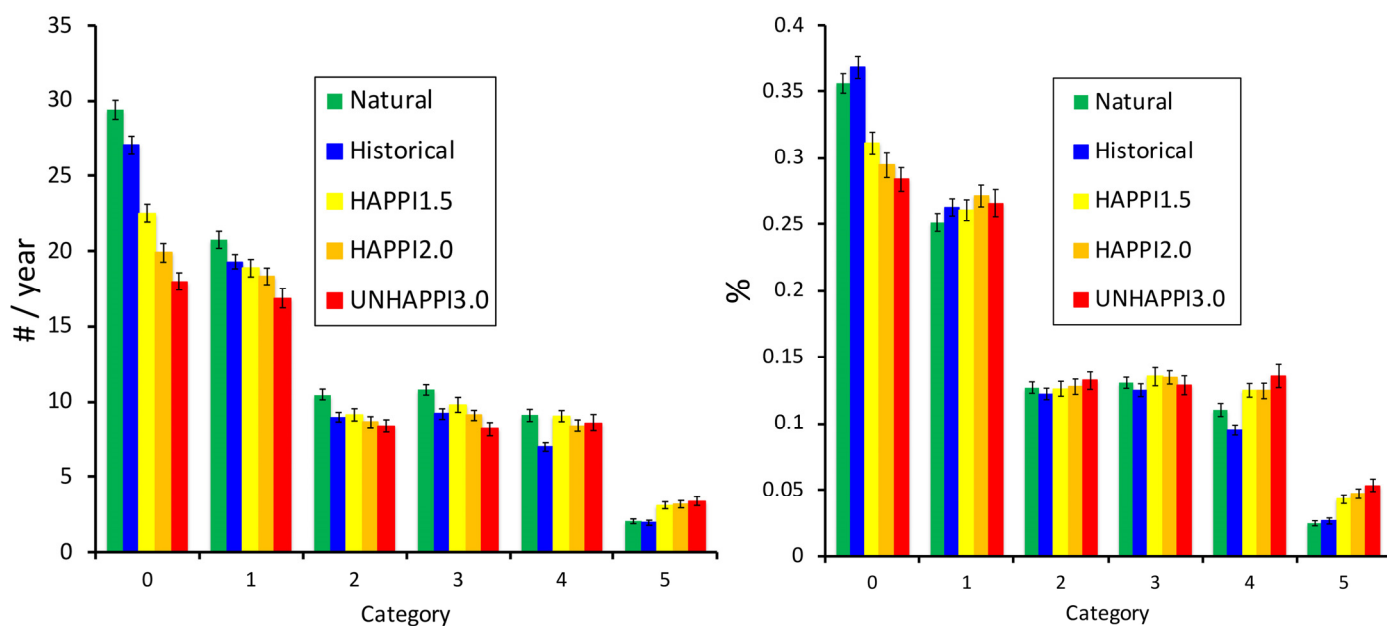

Figure 2. (**Left**) Annual number of tropical storms by category as simulated by CAM5.1 at various global warming levels. (**Right**) Fraction of tropical storms by category as in the left panel. Error bars indicate standard error.

3. Storm Size

Chavas et al., 2015 [33] developed a theoretical model of the radial structure of the low-level tropical cyclone wind field by numerically solving a Riccati equation that relates the radial gradient of the absolute angular momentum and wind speed at a given radius. The spatial distribution of observed storm size from this model using a wind speed of 12 m/s to represent maximum storm extent was shown to agree well with the QuikSCAT Tropical Cyclone Radial Structure database [34]. While this definition of outer storm size radius would provide a good model evaluation metric, here we make a different choice

based on much higher wind speeds to define a metric more relevant to impacts. Table 1 shows the Chavas radius as simulated by the CAM5.1 under present day climate conditions for wind speeds defined as the lower bounds of the Saffir–Simpson categories averaged over all the storms in each of the categories. Averages are performed on the three hourly TECA2 output and aggregated over category at that instant. The table is arranged so that for storm of a given category, average wind speed radii are provided at its strongest rating and for all lower categories. Comparison along the diagonal of Table 1 immediately reveals a model of structural weakness. For all tropical cyclone categories greater than 1, the Chavas radius at its rated wind category is only slightly larger than the climate model's horizontal grid resolution (~25 km). Maximum wind radius is then likely constrained to be close to that resolution and hence any simulated tropical cyclone simply revolves around an eye of a single grid cell. Similar tables for the other CAM5.1 simulations are shown in the supplementary materials.

Table 1. Chavas radius (km) for wind speeds thresholds from the CAM5.1 present day (Historical) simulations as a function of instantaneous Saffir–Simpson categorization. Wind speed thresholds are shown in the second row (m/s). The large volume of data renders standard errors miniscule. The radii (r_n) denote the average radius at wind speeds corresponding to the category n threshold. For instance, the average radius (r_1) of category 4 storms at 33m/s is 62.7 km.

	r_0	r_1	r_2	r_3	r_4	r_5
Wind Speed Threshold (m/s)	18	33	43	50	58	70
Category						
TS (cat 0)	48.3	-	-	-	-	-
1	80.9	31.6	-	-	-	-
2	103.1	41.0	27.7	-	-	-
3	119.8	51.4	34.1	28.6	-	-
4	141.1	62.7	44.6	35.6	29.5	-
5	160.4	73.2	52.4	43.4	34.2	26.7

Despite this resolution limitation of the model presented here (and likely HighResMIP-class models in general), it is informative to examine if climate change introduces any change in tropical cyclone average size. The left panel of Figure 3 reveals that there is no consistent change in the average radii of hurricane force winds (category 1 or 33 m/s) while the right panel reveals similarly for the average radii of major hurricane force winds (category 3 or 50 m/s). A similar conclusion is obtained by examining the Chavas radius tables for various global warming levels in the supplementary materials. Hence, at least in this model, climate change does not alter the average wind speed radial distribution of a simulated tropical cyclone of a specified Saffir–Simpson rating. Further evidence that structure of storms at a specified intensity does not change with warming is provided by examining the relationship between maximum surface wind speed and minimum central pressure, which also was found to be similarly unaffected [24]. In plain language for instance, a category 3 storm in a much warmer future world is not larger nor smaller than a category 3 storm in a preindustrial world despite changes in atmospheric structure, such as lapse rates.

This is not to say that the area impacted by hurricane or major hurricane force winds during an entire season does not change with global warming as storm frequencies at different categories will likely change as, for example, in Figure 2. Furthermore, although high resolution event attribution modeling studies have revealed structural changes in individual tropical cyclones as they are warmed [17], such storms are also intensified, which is not inconsistent with the conclusion shown in Figure 3 or the conclusion drawn above. Hence, while average Chavas radius may be a good model performance metric, it is not by itself a good climate change metric.
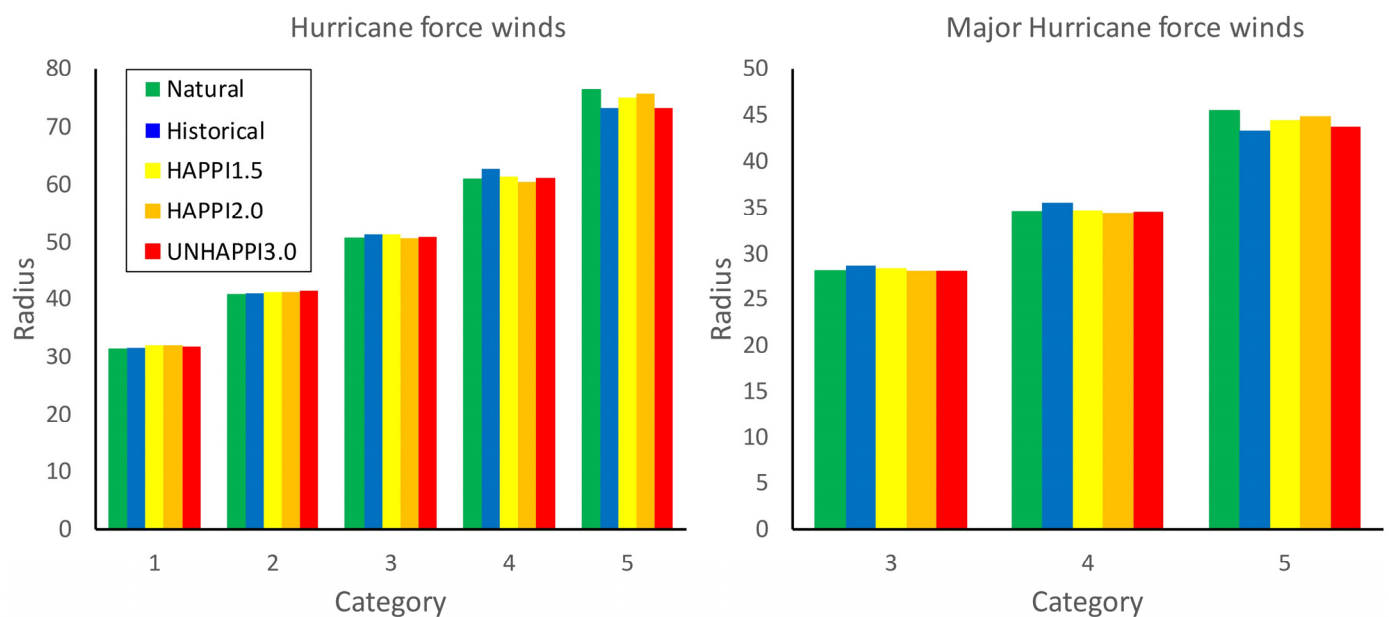
Figure 3. (**Left**) Average radii (km) of hurricane force winds (33 m/s) across Saffir–Simpson categories and global warming levels as simulated by the CAM5.1. (**Right**) Similar but for major hurricane force winds (50 m/s).

4. Accumulated Cyclone Energy Index (ACE)

The accumulated cyclone energy index (ACE) is obtained by summing the square of the peak near surface wind speeds every 6 h over the lifetime of a tropical cyclone. It is commonly used to describe both individual storms as well as seasonal tropical cyclone activity in individual basins or globally. Despite its name, ACE is an index of accumulated pointwise quantities and not a measure of total storm kinetic energy. It is another useful metric, together with storm count, to describe the variations in seasonal tropical cyclone activity. Basin wide ACE statistics have been used as a model validation metric [35] revealing that the CAM5.1 simulated distribution of ACE in North Pacific is skewed toward excess in the eastern part of the basin similar to storm counts [8]. Globally, the present day CAM5.1 simulation is about 20% higher than the observed average over 1995–2015 of 750 ACE units (10^4 knots^2). The left panel of Figure 4 shows global ACE from the CAM5.1 simulations, revealing that present day simulated ACE is both less than in the cooler preindustrial climate and in the warmer future climates amidst substantial uncertainty from interannual variability. This CAM5.1 projection is consistent with similarly inconclusive total global ACE projections [36].
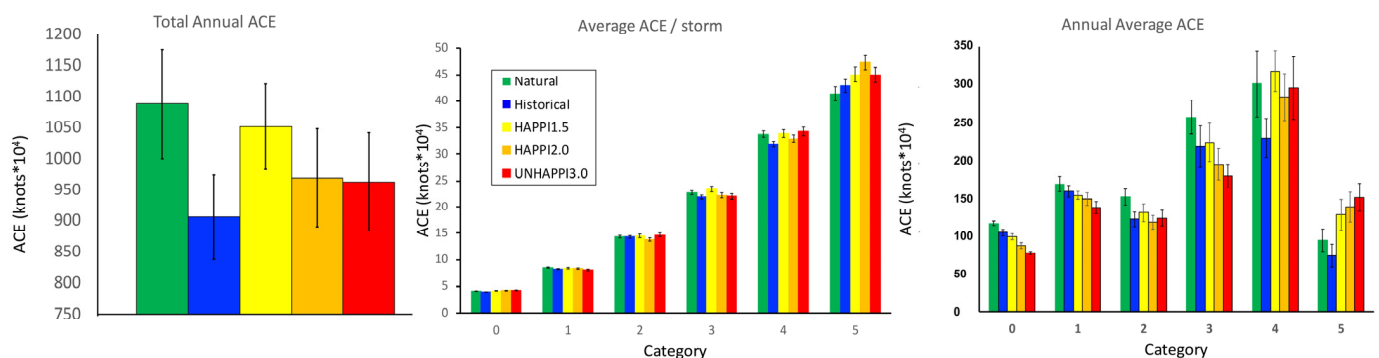

Figure 4. (**Left**) Average annual global accumulated cyclone energy index (ACE) as simulated by CAM5.1 at various global warming levels. Error bars indicate standard error. (**Center**) Average ACE per storm across Saffir–Simpson categories as simulated by CAM5.1 at various global warming levels. (**Right**) Average annual global ACE across Saffir–Simpson categories as simulated in the center panel. Error bars indicate standard error.

The reason for this non-uniform change in average global ACE from one warming level to another is a result of the convolution of changes in tropical cyclone frequency and their distribution across wind speed intensities (Figures 1 and 2). The center panel of Figure 4 shows the average ACE for storms according to their assigned peak category. From tropical storm intensity to category 4, average storm ACE does not change with global warming amount. Similar to the conclusion about this model's storm size from Figure 3 and related tables, climate change does not change the average ACE of storms within these categories. This might be a bit surprising as this model was shown to exhibit longer tropical storm lifetimes with an associated increased poleward track density as the climate warms [24]. However, ACE depends on the square of the instantaneous peak wind speed and the bulk of a storm's ACE is accumulated during its time spent in or near its strongest rated category. This may suggest that the intensification and subsequent decay of tropical cyclones may be unaffected by global warming until late in their lifetimes. However, confidence in this level of detail drawn from a HighResMIP-class model should be very low as this aspect of tropical cyclone development is notoriously difficult to simulate [37]. Average storm ACE within category 5 generally increases with warming as that category is open ended and reflects that the most intense storms become yet more intense with warmer sea surface temperatures. While the UNHAPPI3.0 simulation appears to be an exception, this is also the case with the fewest number of simulated years and the highest uncertainty.

The distribution of simulated annual global average ACE across the Saffir–Simpson categories is shown in the right panel of Figure 4 and reveals that most of the total ACE comes from category 4 storms with the second largest contribution coming from category 3 storms at any global warming level. Changes with warming level in this figure are largely controlled by changes in the tropical cyclone categories counts of Figure 2.

5. Power Dissipation Index (PDI)

The power dissipation index (PDI) is similar to ACE in that it is a (partial) measure of total storm intensity. Instead of accumulating the square of the peak surface wind speed, PDI accumulates the cube of the peak wind speed. Analogous to friction energy applied by flow to a surface, the cube of peak surface wind speed is more closely related to economic damages than tropical cyclone frequency itself [38]. Moreover, similar to ACE, seasonal accumulated PDI will be more influenced by the most intense storms only more so due to the higher nonlinear dependence on peak surface wind speed. Similar to Figure 4, Figure 5 shows annual average global PDI (left), average PDI per storm (center) and average annual global PDI (right) as simulated by the CAM5.1 at various global warming levels. Similar to ACE, the largest contributor to total simulated PDI comes from category 4 storms. However. in this case for the warmer climate conditions, category 5 storms can contribute as much or more to total PDI as category 3 storms reflecting both the intensification of the largest storms and PDI's cubic dependence on peak wind speed.
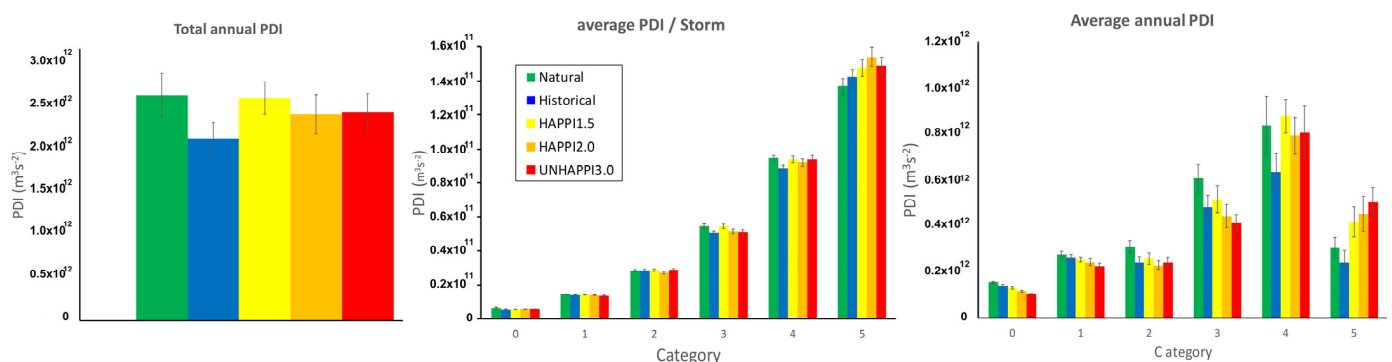

Figure 5. (**Left**) Average annual global power dissipation index (PDI) as simulated by CAM5.1 at various global warming levels. Error bars indicate standard error. (**Center**): Average PDI per storm across Saffir-Simpson categories as simulated by CAM5.1 at various global warming levels. (**Right**) Average annual global PDI across Saffir–Simpson categories as simulated in the center panel. Error bars indicate standard error.

6. Discussion

This study explores global average storm size, accumulated cyclone energy (ACE) and power dissipation index (PDI) as alternatives to simple counting by Saffir-Simpson scale for the detection, attribution and projection of changes in tropical cyclone activity as the planet warms due to anthropogenic influences. As observations are limited, a high resolution (~25 km) global atmospheric general circulation model is used as a tool to examine what changes, if any, might be robust and possibly contained in the actual climate system. While convection permitting models (~4 km or finer) would be a preferable tool for analyzing changes in storm structural statistics, computational constraints preclude the formation of ensemble multi-decadal simulations necessary to extract climate change signals, if any, from the underlying noise.

Simulated changes in the total global annual average ACE and PDI are not found to be robust to global warming. This is largely a result of offsetting changes in overall decreasing storm counts but increasing average intensity. However, it is entirely possible that regional changes in these metrics may be robust if regional changes in storm frequency are substantially different than what they are globally. Indeed, substantial ACE and PDI increases in the North Atlantic have been observed [38,39] and the model exhibits North Atlantic ACE increases but not in the North Pacific [24]. When sorted on the Saffir–Simpson scale, only the highest unbounded category exhibits increased ACE and PDI with warming for the average storm within a category despite an increase in simulated storm duration across categories.

Average instantaneous storm size, as measured by the Chavas radius at surface wind speeds at hurricane (33 m/s) and major hurricane force (50 m/s), is also found not to change with global warming (Figure 3) as might be expected, although model resolution is not high enough to adequately capture eye wall details. Previous studies have focused on average outer storm size, typically measured at 12 m/s or slower [33,40]. Indeed, outer storm size may be a more appropriate detection and attribution metric than the inner radii of Figure 3 as it may be more readily observable and less affected by eyewall processes, although it is less relevant for wind damage impacts. However, climate change projections of average outer storm size are conflicting as Yamada et al. (2017) [41] found an increase with global warming in a 14 km model but Knutson et al. (2015) [42] found no change in the media outer storm size used downscaled CMIP5 models with a 6 km hurricane forecast model. Comparison of r_0 in the first column of Table 1 to that in the tables in the supplementary materials also suggests no change in storm radii at 18 m/s.

There is evidence from event attribution studies that the radial structure of tropical storm precipitation may be affected by global warming [12,17]. However, Figure 3 and the tables show that average radii for each wind speed considered within the Saffir–Simpson categories is not sensitive to global warming. Consistent with previous analyses showing no change with warming in the peak wind speed to pressure minima relationship [24,43,44], this null result suggests that because the wind speed category bounds are relatively narrow, storms for any specified peak wind speed are structurally similar regardless of global warming level. The structural changes seen in event attribution studies are then simply the result in shifts in wind speeds rather than some fundamental structural change. One then might expect a change in the wind speed radii for the unbounded category 5, as only for that category does the average wind speed change with warming. However, the present model's limitations in simulating eyewall processes is especially important when considering such intense storms and the present null result in this case should not be considered definitive.

Dividing global annual average ACE and PDI according to Saffir–Simpson categories yields results very similar to simple counting by categories with general decreases at the lower categories and increases in the highest one. This suggests then that a more robust climate change metric might be exceedances over a high threshold rather than averages. Figure 6 shows the exceedances of each climate scenario over a threshold selected from the historical simulation and reveals little difference between ACE (middle) and PDI

(right). The left panel of Figure 6 shows exceedances of storm peak wind speed. However, this panel is not directly comparable to the other two as is calculated from the storm maximum wind speed over entire storm lifetime and as such is far more extreme than the storm integrated quantities of ACE and PDI. It does not appear that accumulating tropical cyclone intensity metrics over the course of storms and seasons adds significant clarity to disentangling the issue of decreasing storm frequency but increases in the tail of the wind speed distribution.
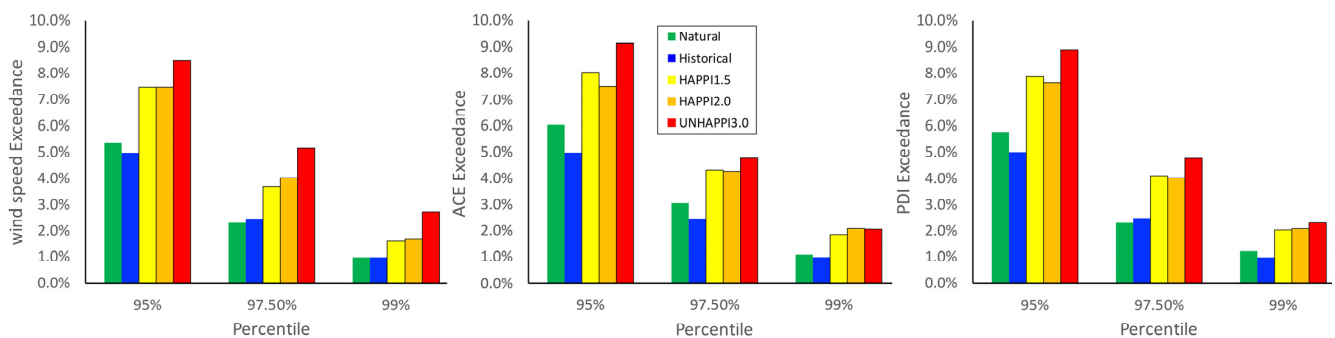
Figure 6. Exceedance over 95, 97.5 and 99th thresholds selected from the Historical CAM5.1 simulation. (**Left**) Maximum storm peak wind. (**Middle**) Storm total ACE. (**Right**) Storm total PDI.

This attempt to find a better metric than global tropical cyclone frequency for climate change detection, attribution and projection produces mixed results. The 6th Assessment Report of the Intergovernmental Panel on Climate Change [45] concluded with high confidence that the fraction of tropical cyclones that achieve category 4 wind speeds or higher would increase with further global warming but made no statement about the number of such intense tropical cyclones. Consistent with Knutson et al. (2019), the assessment recognized that available model projections, including the HighResMIP models, vary greatly in projected decreased global total tropical storm frequency with warming, if any. Hence, if the actual decrease in total tropical storm frequency were to be small and intensification large enough, there would be more intense tropical storms. However, if the decrease in total frequency is large enough, there would be fewer intense tropical storms. Indeed, the trend in intense storm frequency might not even be monotonic with increases at low levels of global warming but decreases at higher levels due to this contention between increased intensification and decreased cyclogenesis. In the context of the current study, this structural uncertainty in future projections of the distribution of tropical storm intensity carries over to future projections of both global ACE and PDI.

While storm size, ACE and PDI are important climate model performance evaluation metrics [16], this combined effect of global warming of decreasing storm count but increasing the intensities of the strongest storms complicates constructing a robust global metric that might exhibit a change given enough data to reduce internal variability. While this study used a climate model that produced between 50 and 100 years of tropical cyclones under stabilized climate scenarios, the real world is a more complex transient system with smaller available data set sizes. Present day exceedance of a contemporary 95th percentile global intensity threshold would result in about four storms annually. Due to the large natural variability of peak tropical storm intensities, confident detection and attribution of the effect of global warming on tropical cyclone intensity statistics relevant to impacts may not be realized with the simple global statistics considered here until far into the future. However, regional versions of these metrics or other even more complex metrics, such as the distribution of storm tracks, storm duration and translational speed, may be more promising.

References

1. Haarsma, R.J.; Roberts, M.J.; Vidale, P.L.; Senior, C.A.; Bellucci, A.; Bao, Q.; Chang, P.; Corti, S.; Fučkar, N.S.; Guemas, V.; et al. High resolution model intercomparison project (HighResMIP v1.0) for CMIP6. geosci. *Model Dev.* **2016**, *9*, 4185–4208. [CrossRef]
2. Wehner, M.F.; Bala, G.; Duffy, P.; Mirin, A.A.; Romano, R. Towards direct simulation of future tropical cyclone statistics in a high-resolution global atmospheric model. *Adv. Meteorol.* **2010**, *2010*, 915303. [CrossRef]
3. Reed, K.A.; Bacmeister, J.T.; Rosenbloom, N.A.; Wehner, M.F.; Bates, S.C.; Lauritzen, P.H.; Truesdale, J.E.; Hannay, C. Impact of the dynamical core on the direct simulation of tropical cyclones in a high-resolution global model. *Geophys. Res. Lett.* **2015**, *42*, 3603–3608. [CrossRef]
4. Strachan, J.; Vidale, P.L.; Hodges, K.; Roberts, M.; Demory, M.-E. Investigating global tropical cyclone activity with a hierarchy of AGCMs: The role of model resolution. *J. Clim.* **2013**, *26*, 133–152. [CrossRef]
5. Roberts, M.J.; Camp, J.; Seddon, J.; Vidale, P.L.; Hodges, K.; Vanniere, B.; Mecking, J.; Haarsma, R.; Bellucci, A.; Scoccimarro, E.; et al. Impact of model resolution on tropical cyclone simulation using the HighResMIP–PRIMAVERA multimodel ensemble. *J. Clim.* **2020**, *33*, 2557–2583. [CrossRef]
6. Murakami, H.; Vecchi, G.A.; Underwood, S.; Delworth, T.L.; Wittenberg, A.T.; Anderson, W.G.; Chen, J.H.; Gudgel, R.G.; Harris, L.M.; Lin, S.J.; et al. Simulation and prediction of category 4 and 5 hurricanes in the high-resolution GFDL HiFLOR coupled climate model. *J. Clim.* **2015**, *28*, 9058–9079. [CrossRef]
7. Reed, K.A.; Jablonowski, C. Impact of physical parameterizations on idealized tropical cyclones in the Community Atmosphere Model. *Geophys. Res. Lett.* **2011**, *38*. [CrossRef]
8. Wehner, M.F.; Reed, K.A.; Li, F.; Bacmeister, J.; Chen, C.-T.; Paciorek, C.; Gleckler, P.; Sperber, K.; Collins, W.D.; Andrew, G.; et al. The effect of horizontal resolution on simulation quality in the Community Atmospheric Model, CAM5.1. *J. Adv. Model. Earth Syst.* **2014**, *6*, 980–997. [CrossRef]

9. Satoh, M.; Tomita, H.; Yashiro, H.; Kajikawa, Y.; Miyamoto, Y.; Yamaura, T.; Miyakawa, T.; Nakano, M.; Kodama, C.; Noda, A.T.; et al. Outcomes and challenges of global high-resolution non-hydrostatic atmospheric simulations using the K computer. *Prog. Earth Planet. Sci.* **2017**, *4*, 13. [CrossRef]

10. Knutson, T.; Camargo, S.J.; Chan, J.C.L.; Emanuel, K.; Ho, C.-H.; Kossin, J.; Mohapatra, M.; Satoh, M.; Sugi, M.; Walsh, K.; et al. Tropical cyclones and climate change assessment: Part I: Detection and attribution. *Bull. Am. Meteorol. Soc.* **2020**, *100*, 1987–2007. [CrossRef]

11. Knutson, T.; Camargo, S.J.; Chan, J.C.L.; Emanuel, K.; Ho, C.-H.; Kossin, J.; Mohapatra, M.; Satoh, M.; Sugi, M.; Walsh, K.; et al. Tropical Cyclones and Climate Change Assessment: Part II. Projected Response to Anthropogenic Warming. *Bull. Am. Meteorol. Soc.* **2019**, *101*, E303–E322. [CrossRef]

12. Reed, K.A.; Stansfield, A.M.; Wehner, M.F.; Zarzycki, C.M. Forecasted attribution of the human influence on Hurricane Florence. *Sci. Adv.* **2020**, *6*. [CrossRef] [PubMed]

13. van Oldenborgh, G.J.; van der Wiel, K.; Sebastian, A.; Singh, R.; Arrighi, J.; Otto, F.; Haustein, K.; Li, S.; Vecchi, G.; Cullen, H. Attribution of extreme rainfall from Hurricane Harvey, August 2017. *Environ. Res. Lett.* **2017**, *12*, 124009. [CrossRef]

14. Wang, S.Y.S.; Zhao, L.; Yoon, J.H.; Klotzbach, P.; Gillies, R.R. Quantitative attribution of climate effects on Hurricane Harvey's extreme rainfall in Texas. *Environ. Res. Lett.* **2018**. [CrossRef]

15. Risser, M.D.; Wehner, M.F. Attributable human-induced changes in the likelihood and magnitude of the observed extreme precipitation during hurricane harvey. *Geophys. Res. Lett.* **2017**, *44*, 12457–12464. [CrossRef]

16. Zarzycki, C.M.; Ullrich, P.A.; Reed, K.A. Metrics for Evaluating Tropical Cyclones in Climate Data. *J. Appl. Meteorol. Climatol.* **2021**, *60*, 643–660. [CrossRef]

17. Patricola, C.M.; Wehner, M.F. Anthropogenic influences on major tropical cyclone events. *Nature* **2018**, *563*, 339–346. [CrossRef]

18. Stansfield, A.M.; Reed, K.A.; Zarzycki, C.M.; Ullrich, P.A.; Chavas, D.R. Assessing Tropical Cyclones' Contribution to Precipitation over the Eastern United States and Sensitivity to the Variable-Resolution Domain Extent. *J. Hydrometeorol.* **2020**, *21*, 1425–1445. [CrossRef]

19. Min, S.-K.; Zhang, X.; Zwiers, F.W.; Hegerl, G.C. Human contribution to more-intense precipitation extremes. *Nature* **2011**, *470*, 378. [CrossRef]

20. Zhang, X.; Wan, H.; Zwiers, F.W.; Hegerl, G.C.; Min, S.-K. Attributing intensification of precipitation extremes to human influence. *Geophys. Res. Lett.* **2013**, *40*, 5252–5257. [CrossRef]

21. Takayabu, I.; Hibino, K.; Sasaki, H.; Shiogama, H.; Mori, N.; Shibutani, Y.; Takemi, T. Climate change effects on the worst-case storm surge: A case study of Typhoon Haiyan. *Environ. Res. Lett.* **2015**, *10*, 064011. [CrossRef]

22. Wehner, M.F.; Reed, K.A.; Zarzycki, C.M. High-resolution multi-decadal simulation of tropical cyclones, Hurricanes and Climate Change. In *Hurricanes and Climate Change*; Springer: Cham, Switzerland, 2017. [CrossRef]

23. Oouchi, K.; Yoshimura, J.; Yoshimura, H.; Mizuta, R.; Kusonoki, S.; Noda, A. Tropical cyclone climatology in a global-warming climate as simulated in a 20 km-mesh global atmospheric model: Frequency and wind intensity analyses. *J. Meteorol. Soc. Japan. Ser. II* **2006**, *84*, 259–276. [CrossRef]

24. Wehner, M.F.; Reed, K.A.; Loring, B.; Stone, D.; Krishnan, H. Changes in tropical cyclones under stabilized 1.5 and 2.0 °C global warming scenarios as simulated by the Community Atmospheric Model under the HAPPI protocols. *Earth Syst. Dyn.* **2018**, *9*, 187–195. [CrossRef]

25. Bhatia, K.; Vecchi, G.; Murakami, H.; Underwood, S.; Kossin, J. Projected response of tropical cyclone intensity and intensification in a global climate model. *J. Clim.* **2018**, *31*, 8281–8303. [CrossRef]

26. Bloemendaal, N.; de Moel, H.; Mol, J.M.; Bosma, P.R.M.; Polen, A.N.; Collins, J.M. Adequately reflecting the severity of tropical cyclones using the new Tropical Cyclone Severity Scale. *Environ. Res. Lett.* **2021**, *16*, 14048. [CrossRef]

27. Bosma, C.D.; Wright, D.B.; Nguyen, P.; Kossin, J.P.; Herndon, D.C.; Shepherd, J.M. An Intuitive Metric to Quantify and Communicate Tropical Cyclone Rainfall Hazard. *Bull. Am. Meteorol. Soc.* **2020**, *101*, E206–E220. [CrossRef]

28. Song, J.Y.; Alipour, A.; Moftakhari, H.R.; Moradkhani, H. Toward a more effective hurricane hazard communication. *Environ. Res. Lett.* **2020**, *15*, 64012. [CrossRef]

29. Bacmeister, J.T.; Wehner, M.F.; Neale, R.B.; Gettelman, A.; Hannay, C.; Lauritzen, P.H.; Caron, J.M.; Truesdale, J.E. Exploratory high-resolution climate simulations using the community atmosphere model (CAM). *J. Clim.* **2014**, *27*, 3073–3099. [CrossRef]

30. Stone, D.A.; Christidis, N.; Folland, C.; Perkins-Kirkpatrick, S.; Perlwitz, J.; Shiogama, H.; Wehner, M.F.; Wolski, P.; Cholia, S.; Krishnan, H.; et al. Experiment design of the international CLIVAR C20C+ detection and attribution project. *Weather Clim. Extrem.* **2019**, *24*, 100206. [CrossRef]

31. Mitchell, D.; AchutaRao, K.; Allen, M.; Bethke, I.; Beyerle, U.; Ciavarella, A.; Forster, P.M.; Fuglestvedt, J.; Gillett, N.; Haustein, K.; et al. Half a degree additional warming, prognosis and projected impacts (HAPPI): Background and experimental design. *Geosci. Model Dev.* **2017**, *10*, 571–583. [CrossRef]

32. Prabhat; Rübel, O.; Byna, S.; Wu, K.; Li, F.; Wehner, M.; Bethel, W. TECA: A parallel toolkit for extreme climate analysis. In *Procedia Computer Science*; Elsevier: Amsterdam, The Netherlands, 2012. [CrossRef]

33. Chavas, D.R.; Lin, N.; Emanuel, K. A model for the complete radial structure of the tropical cyclone wind field. Part I: Comparison with observed structure. *J. Atmos. Sci.* **2015**, *72*, 3647–3662. [CrossRef]

34. Chavas, D.R.; Lin, N.; Dong, W.; Lin, Y. Observed tropical cyclone size revisited. *J. Clim.* **2016**, *29*, 2923–2939. [CrossRef]

35. Shaevitz, D.A.; Camargo, S.J.; Sobel, A.H.; Jonas, J.A.; Kim, D.; Kumar, A.; Larow, T.E.; Lim, Y.-K.; Murakami, H.; Reed, K.A.; et al. Characteristics of tropical cyclones in high-resolution models in the present climate. *J. Adv. Model. Earth Syst.* **2014**, *6*. [CrossRef]

36. Guimarães, S.O. Climate models accumulated cyclone energy analysis. In *Current Topics in Tropical Cyclone Research*; Lupo, A., Ed.; IntechOpen: London, UK, 2020. [CrossRef]

37. Judt, F.; Chen, S.S. Predictability and dynamics of tropical cyclone rapid intensification deduced from high-resolution stochastic ensembles. *Mon. Weather Rev.* **2016**, *144*, 4395–4420. [CrossRef]

38. Emanuel, K. Increasing destructiveness of tropical cyclones over the past 30 years. *Nature* **2005**, *436*, 686–688. [CrossRef]

39. Murakami, H.; Li, T.; Hsu, P.C. Contributing factors to the recent high level of accumulated cyclone energy (ACE) and power dissipation index (PDI) in the North Atlantic. *J. Clim.* **2014**, *27*, 3023–3034. [CrossRef]

40. Chavas, D.R.; Reed, K.A. Dynamical aquaplanet experiments with uniform thermal forcing: System dynamics and implications for tropical cyclone genesis and size. *J. Atmos. Sci.* **2019**, *76*, 2257–2274. [CrossRef]

41. Yamada, Y.; Satoh, M.; Sugi, M.; Kodama, C.; Noda, A.T.; Nakano, M.; Nasuno, T. Response of tropical cyclone activity and structure to global warming in a high-resolution global nonhydrostatic model. *J. Clim.* **2017**, *30*, 9703–9724. [CrossRef]

42. Knutson, T.R.; Sirutis, J.J.; Zhao, M.; Tuleya, R.E.; Bender, M.; Vecchi, G.A.; Villarini, G.; Chavas, D. Global Projections of Intense Tropical Cyclone Activity for the Late Twenty-First Century from Dynamical Downscaling of CMIP5/RCP4.5 Scenarios. *J. Clim.* **2015**, *28*, 7203–7224. [CrossRef]

43. Chavas, D.R.; Reed, K.A.; Knaff, J.A. Physical understanding of the tropical cyclone wind-pressure relationship. *Nat. Commun.* **2017**, *8*, 1360. [CrossRef]

44. Satoh, M.; Yamada, Y.; Sugi, M.; Komada, C.; Noda, A.T. Constraint on future change in global frequency of tropical cyclones due to global warming. *J. Meteorol. Soc. Jpn. Ser. II* **2015**, *93*, 489–500. [CrossRef]

45. Seneviratne, S.I.; Zhang, X.; Adnan, M.; Badi, W.; Dereczynski, C.; di Luca, A.; Ghosh, S.; Iskandar, I.; Kossin, J.; Lewis, S.; et al. Weather and Climate Extreme Events in a Changing Climate. In *Climate Change 2021: The Physical Science Basis. Contribution of Working Group I to the Sixth Assessment Report of the Intergovern-Mental Panel on Climate Change*; Masson-Delmotte, V., Zhai, P., Pirani, A., Connors, S.L., Péan, C., Berger, S., Caud, N., Chen, Y., Goldfarb, L., Gomis, M.I., et al., Eds.; Cambridge University Press: Cambridge, UK, 2021, in press.